High gain optical parametric amplification in ultra-silicon-rich nitride (USRN) waveguides

High gain optical parametric amplification in ultra-silicon-rich nitride (USRN) waveguides

K. J. A. Ooi, D. K. T. Ng, J. W. Choi, E. Sahin, P. Xing, et al.

K. J. A. Ooi, D. K. T. Ng, J. W. Choi, E. Sahin, P. Xing, T. Wang, A. K. L. Chee, L. C. Kimerling, A. M. Agarwal, D. T. H. Tan, "High gain optical parametric amplification in ultra-silicon-rich nitride (USRN) waveguides," Proc. SPIE 10684, Nonlinear Optics and its Applications 2018, 1068406 (14 May 2018); doi: 10.1117/12.2306238

Event: SPIE Photonics Europe, 2018, Strasbourg, France

High gain optical parametric amplification in ultra-silicon-rich nitride (USRN) waveguides

K. J. A. Ooi[a], D. K. T. Ng[b], J. W. Choi[a], E. Sahin[a], P. Xing[a], T. Wang[a], A. K. L. Chee[c], L. C. Kimerling[c], A. M. Agarwal[c] and D. T. H. Tan[a,*]
[a]SUTD-MIT International Design Center, Singapore University of Technology and Design, 8 Somapah Road, 487372 Singapore;
[b]Data Storage Institute, Agency for Science, Technology and Research (A*STAR), 2 Fusionopolis Way, #08-01 Innovis, 138634 Singapore.
[c]Department of Materials Science and Engineering, Massachusetts Institute of Technology, 77 Massachusetts Avenue, Cambridge, Massachusetts 02139, USA.
*dawn_tan@sutd.edu.sg

ABSTRACT

Optical parametric amplifiers rely on the high Kerr nonlinearities and low two-photon absorption (TPA) to achieve large optical amplification. The high Kerr nonlinearity enables efficient energy transfer from the optical pump to the signal. On the other hand, the TPA process competes with the amplification process, and thus should be eliminated. Through Miller's rule and Kramers-Kronig relations, it is known that the material's Kerr nonlinearity scales inversely proportional to the band-gap, while the TPA process occurs when the photon energy is larger than the band-gap energy and Urbach tails, thus presenting a trade-off scenario. Based on these requirements, we have designed a CMOS-compatible, band-gap engineered nitride platform with ultra-rich silicon content. The silicon nitride material is compositionally engineered to have a band-gap energy of 2.1 eV, which is low enough to confer a high Kerr nonlinearity, but still well above the energy required for the TPA process to occur. The new material, which we called ultra-silicon-rich nitride (USRN), has a material composition of Si_7N_3, a high Kerr nonlinearity of 2.8×10^{-13} cm^2/W, and a negligible TPA coefficient. In optical amplification experiments, 500 fs pulses at 14 W peak power and centered around 1560 nm are combined with continuous wave signals. The maximum parametric gain of the signal could reach 42.5 dB, which is one of the largest gains demonstrated on CMOS platforms to date. Moreover, cascaded four-wave mixing down to the third idler, which was usually observed for mid-infrared silicon waveguides, is unprecedentedly observed at this spectrum.

Keywords: Ultra-silicon-rich nitride, Band-gap Engineering, Nonlinear Optics, Photonic Crystal Waveguides, Optical Parametric Amplification, CMOS Photonics

1. INTRODUCTION

Optical parametric amplifiers rely on the inherent nonlinearity of the host medium to achieve optical amplification. The amplified signals scale quadratically with the pump power, enabling extremely large amplification factors. Optical parametric amplification with high gain is therefore highly sought after, as it is one of the most efficient methods for amplifying light and achieving high powered optical fields. Large optical nonlinearities and negligible nonlinear losses are ideal for such processes, as they enable the parametric process to occur efficiently using low power. In addition to the Kerr nonlinearity of the material, two-photon absorption (TPA) which compete with the amplification process need to be kept to a minimum. From Miller's rule and Kramers-Kronig relations[1,2], it is known and observed that when the silicon-content of silicon nitride is increased, the linear refractive index increases, the bandgap decreases, and hence the Kerr nonlinearity is increased. Indeed, Figure 1 demonstrates how a CMOS material could be band-gap engineered to the Urbach edge of the TPA to obtain the maximum Kerr nonlinearity without TPA losses[3]. From the collection of experimental data of various amorphous CMOS materials, we see a clear scaling rule that follows a log-linear relationship between the Kerr nonlinear index and the linear refractive index.

Nonlinear Optics and its Applications 2018, edited by Benjamin J. Eggleton, Neil G. R. Broderick, Anna C. Peacock
Proc. of SPIE Vol. 10684, 1068406 · © 2018 SPIE · CCC code: 0277-786X/18/$18 · doi: 10.1117/12.2306238

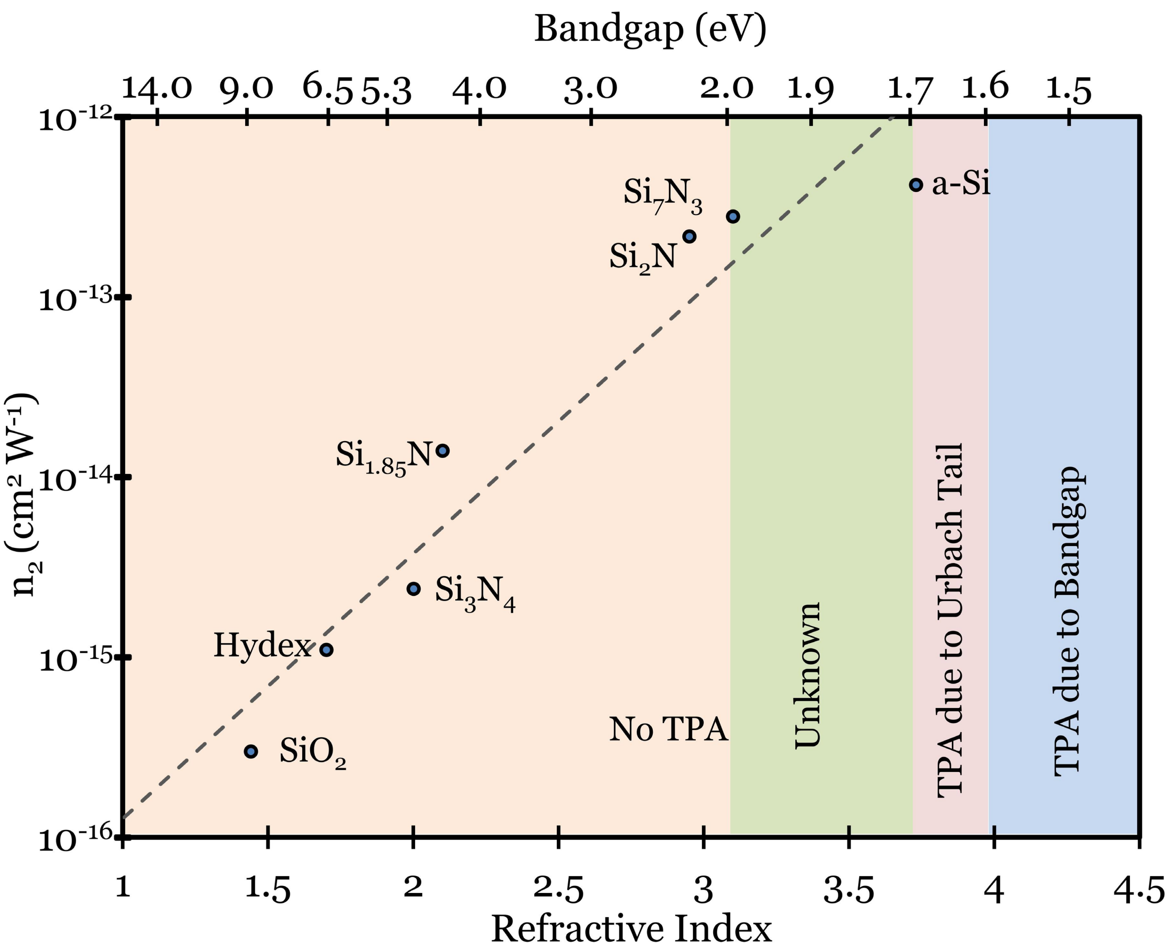

Figure 1 The optical Kerr nonlinear refractive index relationship with the linear refractive index of various amorphous CMOS materials sits on a log-linear scaling rule as denoted by the dotted line[3]. The corresponding bandgap values are fitted empirically from experimental reported values[3-12]. The highest Kerr nonlinearity achievable, without the associated TPA losses, is USRN at a refractive index of 3.1. Amorphous silicon, at a refractive index of 3.7, has a higher Kerr nonlinearity but with significant TPA losses due to the presence of Urbach tails. Amorphous CMOS materials with refractive indices from 3.1 to 3.6 are yet to be discovered.

In this work, we engineer ultra-rich-silicon nitride (USRN) which has a material composition of Si_7N_3[3-6]. USRN possesses a significantly higher Kerr nonlinearity of $2.8x10^{-13}$ cm^2/W, and a negligible TPA coefficient, as compared to other compositions of silicon nitride[7-9]. We demonstrate ultra-high optical parametric amplification on the USRN platform – as large as 42.5 dB on a sub-centimeter waveguide – which is one of the largest gains demonstrated on CMOS platforms to date[1]. Moreover, cascaded four-wave mixing down to the third idler is unprecedentedly observed at this spectrum. This is usually observed in silicon waveguides at the mid-infrared but not at the telecommunications wavelength. We have observed a respected 7.7 dB gain for the third idler, alongside with 21.2 dB for the second idler, and 36.2 dB for the first idler.

2. DESIGN, FILM DEPOSITION, AND FABRICATION OF HIGHLY NONLINEAR ULTRA-RICH-SILICON NITRIDE OPTICAL WAVEGUIDES

2.1 Film deposition

Ultra-silicon-rich nitride (USRN) films, in the ratio of Si:N = 7:3, are deposited using inductively-coupled plasma chemical vapour deposition and they have a band gap of 2.05 eV – large enough to eliminate two photon absorption, including that from the Urbach band tail states. USRN films are deposited at a low temperature of 250^{o}C, making them suitable for back-end CMOS processing. Precursor gases used are SiH_4 and N_2, while NH_3 is intentionally avoided as it is likely to generate unwanted N-H bonds which have absorption peaks close to the 1.55 μm wavelength. These films turn out to have a high Kerr nonlinear coefficient of 2.8×10^{-13} cm^2 W^{-1}, with no observable TPA losses[5].

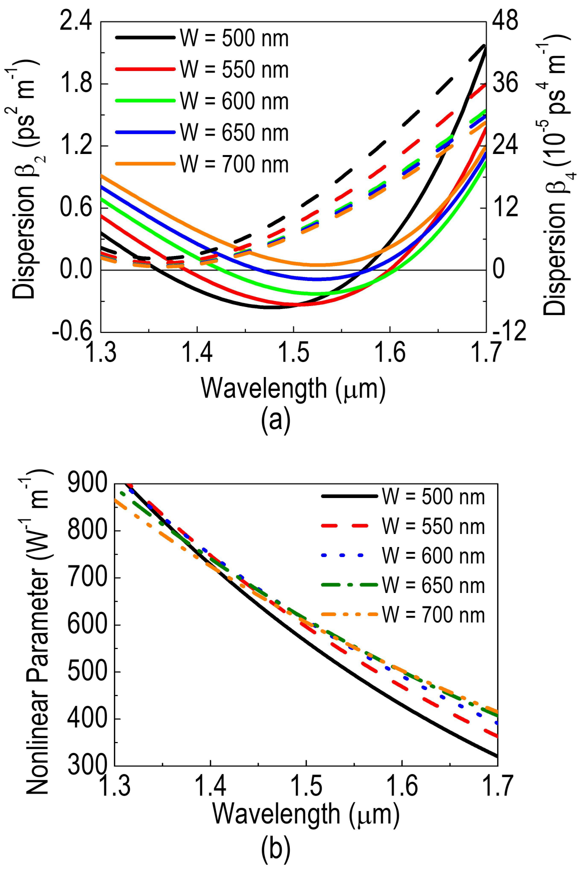

Figure 2 (a) Dispersion and (b) nonlinear parameter engineering and optimization of USRN waveguides. The dispersion is calculated for the second-order (solid lines) and fourth-order (dashed lines) for different waveguide widths and for a fixed film thickness of 300 nm. The nonlinear parameter is also optimized in the waveguide design.

2.2 Waveguide dispersion engineering

From the USRN films, waveguides optimized for low dispersion are fabricated. Preferably, the nonlinear waveguide has to be operated near the zero-dispersion wavelength in order to maximise phase-matching between the pump and signal, so as to maximise conversion efficiency and optical gain. Figure 2 shows the dispersion and nonlinear parameter design from mode simulations and numerical calculations. The dispersion of the USRN waveguides is calculated up to the fourth-order in order to obtain the accurate phase-matching conditions. Meanwhile, the nonlinear parameter also plays a role to ensure a high optical confinement in the USRN waveguide to obtain a high conversion efficiency. From the calculated results in Figure 2, we determined the design with the most optimized dispersion profile and nonlinearity to be 550 nm × 300 nm.

3. OPTICAL PARAMETRIC AMPLIFICATION AND FOUR-WAVE MIXING EXPERIMENTS

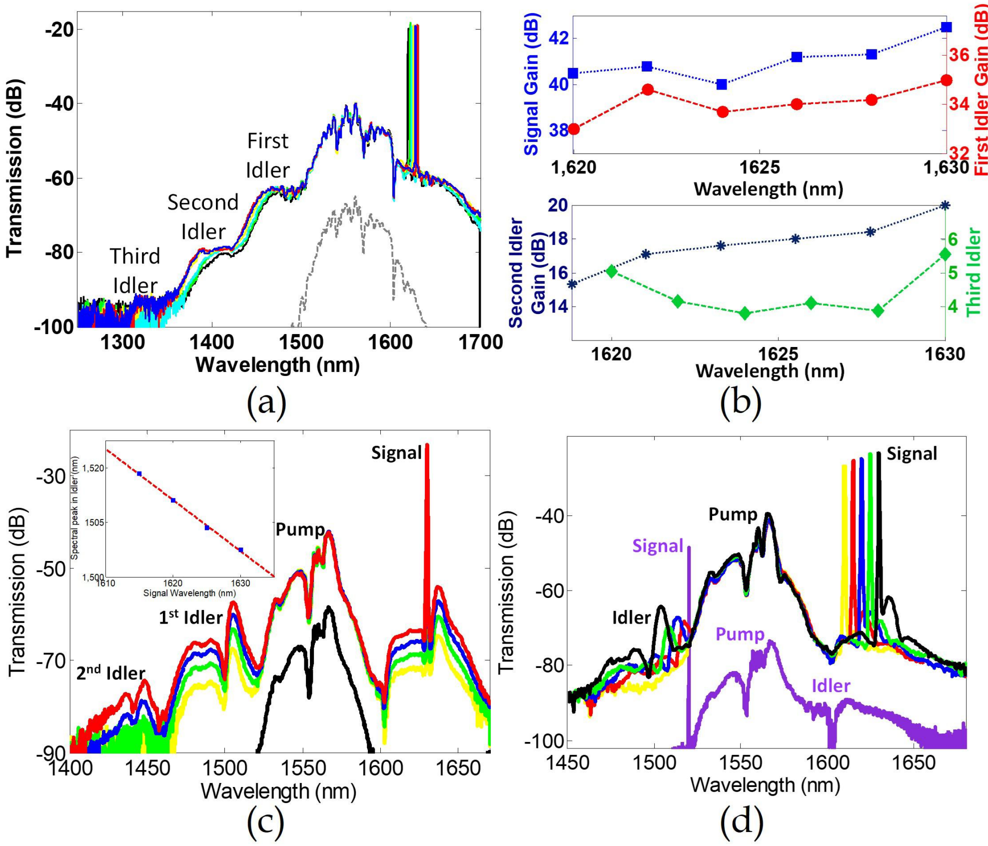

Figure 3 (a) Optical parametric amplification using a 500 fs pulse experiment. (b) Measured signal and idler parametric gain. As high as 42 dB signal gain is achieved. (c) Optical parametric amplification using a 2.0 ps pulse experiment. (d) Measured four wave mixing spectra when signal wavelength is tuned from 1610-1630 nm and 1520 nm. Four-wave mixing transmission spectra, where spectral feature at 1400-1450nm represents evidence of cascaded four-wave mixing

500 fs pulses centered at 1560 nm with a peak power of 14 W are combined with a continuous wave signal (power fixed at 40 μW) using a wavelength division multiplexer. The signal wavelengths are varied from 1620-1630 nm and the generated four-wave mixing spectra is shown in Figure 3(a). Analyses of the on/off optical parametric gain experienced by the signal and idlers are performed as shown in Figure 3(b). The maximum parametric gain experienced by the signal and first idler is 42.5 dB and 36.2 dB respectively. This signal gain to our knowledge, represents the largest demonstrated to date on a CMOS compatible platform. The absence of any observable build-up of photo-excited free carriers in the mixing of the pulsed pump and continuous wave signal implies that the demonstrated nonlinear effects are intrinsically ultrafast.

We also investigate parametric amplification of longer pulses. In a second set of experiments, we use pulses with a temporal duration of 2.0 ps centered at 1560 nm, and a peak pump power of 10 W, for four wave mixing experiments. In the regime of negligible nonlinear losses, the parametric gain should remain unchanged when the pulse width is varied (from 500 fs to 2.0 ps), but peak power is maintained. Figure 3(c) shows the measured four-wave mixing spectra including the observation of cascaded four-wave mixing up to the second idler. Meanwhile, Figure 3(d) shows the four-wave mixing spectra when the signal wavelength is tuned. For these experiments, a peak parametric gain of 30 dB is achieved for the amplified signals.

4. EHNHANCING OPTICAL NONLINEARITY OF USRN WAVEGUIDES WITH RESONANT AND SLOW-WAVE STRUCTURES

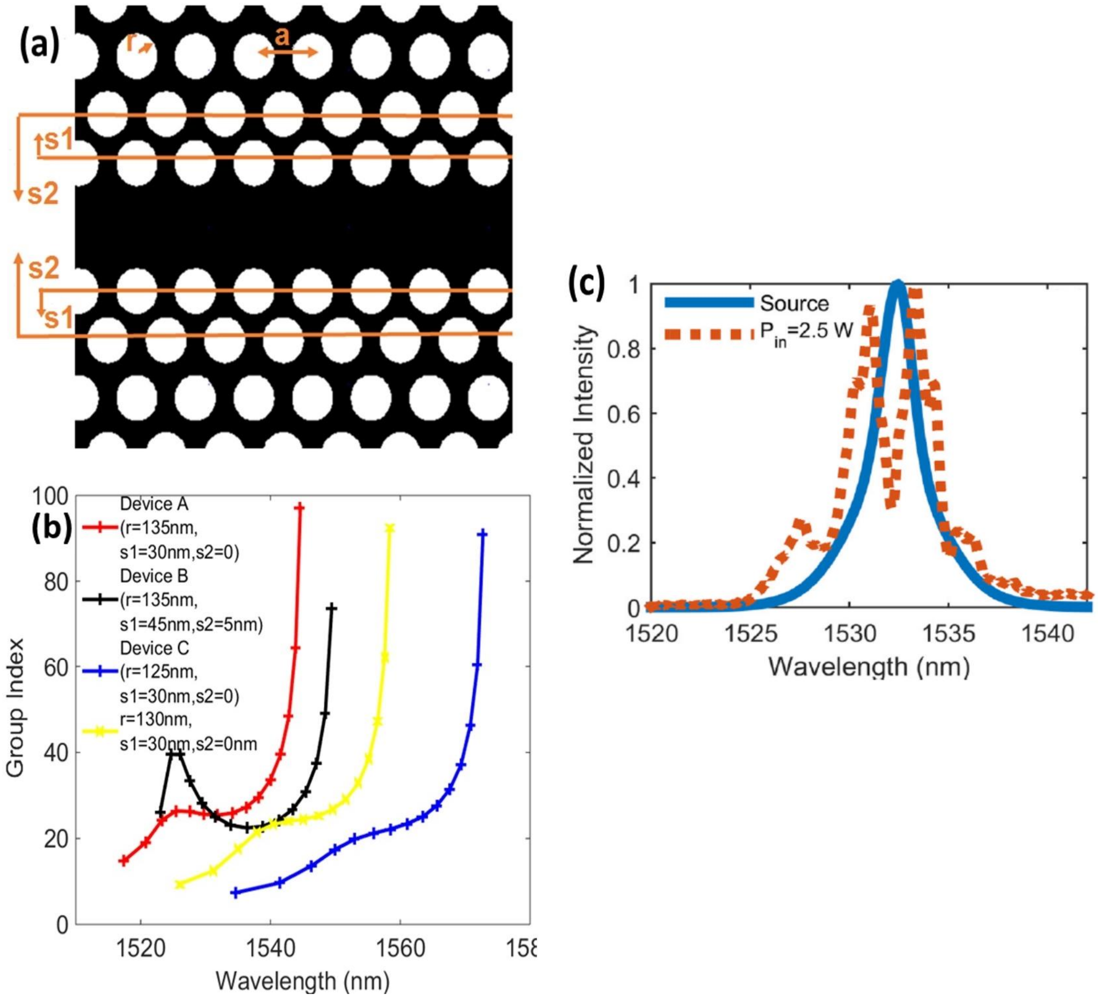

Figure 4 (a) Design of USRN flat-band photonic crystal waveguides by method of row shifting. (b) Group index curves for 3 devices with various row-shifts. (c) Self-phase modulation spectra for Device C.

The nonlinearity of waveguides could be further enhanced using resonant or slow-wave structures, so as to enable the prolonged interaction of light with the material[13-16]. For USRN waveguides, we have designed flat-band photonic crystal waveguides (PhCW) for this purpose[13]. Using a systematic row-shifting method as depicted in Figure 4(a)[17,18], we have designed 3 PhCW devices with different flat-band group indices as shown in Figure 4(b). Using Device C as an example, it has a flat-band group index of ~19 over the bandwidth of 5 nm. For this device, self-phase modulation experiments were conducted, with parameters of 1.9ps pulses, 96.6 μm PhCW length, and peak pump power of 2.5 W. From Figure 4(c), we observe a 1.5 π phase acquisition, which translates to an effective nonlinear parameter of 1.97×10^4 $(Wm)^{-1}$.

5. PERFORMANCE COMPARISON OF NONLINEAR AMORPHOUS CMOS OPTICAL PLATFORMS

Table 1 presents a performance comparison of the various CMOS-compatible material platforms. It is straightforward to compare the nonlinear refractive index, the nonlinear parameter and the TPA coefficient as the trends can already be seen from Figure 1. However, the current biggest issue with USRN waveguide is the substantial propagation losses.

While material losses are determined to be negligible from measurements, the propagation losses have likely arisen from the sidewall roughness of the waveguide. Further fabrication process optimization would be required in order to reduce these propagation losses.

Table 1. Comparison of Key Performance Indicators for various nonlinear amorphous CMOS optical platforms

	a-Si[12]	Hydex[11]	Si_3N_4[7]	$Si_{1.85}N$[9]	$Si_{1.25}N$[10]	Si_2N[8]	Si_7N_3[3-6]
n_2 (cm^2/W)	4.2×10^{-13}	1.1×10^{-15}	2.4×10^{-15}	1.4×10^{-14}	1.6×10^{-14}	1.6×10^{-13}	2.8×10^{-13}
γ (W^{-1}/m)	1200	0.25	0.65	6.1	16	206	430–550
β_{TPA} (cm GW^{-1})	0.25	nil	nil	nil	nil	nil	nil
Propagation Loss (dB/cm)	~4.5	0.06	8×10^{-4}	~1	1.5	~1	1.9 - 4.5
$\gamma.L_{eff,max}$(W^{-1})	11.6	0.18	3.5	0.27	0.46	8.9	4.8 – 9.8

ACKNOWLEDGMENTS

This work was supported by the MOE ACRF Tier 2 grant, National Research Foundation Competitive Research Grant, SUTD-MIT International Design center, and Temasek Laboratories grant. The authors acknowledge the National Research Foundation, Prime Minister's Office, Singapore, under its Medium Sized Centre Program

REFERENCES

[1] Lucarini, V., Saarinen, J. J., Peiponen, K. E. and Vartiainen, E. M., [Kramers-Kronig Relations in Optical Materials Research], Springer, Berlin (2005).

[2] Miller, R. C., "Optical second harmonic generation in piezoelectric crystals," Appl. Phys. Lett. 5, 17-19 (1964).

[3] Ooi, K. J. A., et al., "Pushing the limits of CMOS optical parametric amplifiers with USRN: Si_7N_3 above the two-photon absorption edge," Nat. Commun. 8, 13878 (2017).

[4] Wang, T., et al., "Supercontinuum generation in bandgap engineered, back-end CMOS compatible silicon rich nitride waveguides," Laser Photonics Rev. 9, 498−506 (2015).

[5] Ng, D. K. T., et al., "Exploring high refractive index silicon-rich nitride films by low-temperature inductively coupled plasma chemical vapor deposition and applications for integrated waveguides," ACS Appl. Mat. Interfaces 7, 21884–21889 (2015).

[6] Choi, J. W., Chen, G. F. R., Ng, D. K. T., Ooi, K. J. A. and Tan, D. T. H., "Wideband nonlinear spectral broadening in ultra-short ultra - silicon rich nitride waveguides," Sci. Rep. 6, 27120 (2016).

[7] Tan, D. T. H., Ikeda, K., Sun, P. C. and Fainman, Y., "Group velocity dispersion and self-phase modulation in silicon nitride waveguides," Appl. Phys. Lett. 96, 061101 (2010).

[8] Lin, G. R., et al., "Si-rich SiNx based Kerr switch enables optical data conversion up to 12 Gbit/s," Sci. Rep. 5, 9611 (2015).

[9] Krückel, C. J., et al., "Linear and nonlinear characterization of low-stress high-confinement silicon-rich nitride waveguides," Opt. Express 23, 25827-25837 (2015).

[10] Lacava, C., et al., "Si-rich silicon nitride for nonlinear signal processing applications," Sci. Rep. 7, 22 (2017).

[11] Ferrera, M., et al., "Low-power continuous-wave nonlinear optics in doped silica glass integrated waveguide structure," Nat. Photonics 2, 737–740 (2008).

[12] Kuyken, B., et al., "On-chip parametric amplification with 26.5 dB gain at telecommunication wavelengths using CMOS-compatible hydrogenated amorphous silicon waveguides," Opt. Lett. 36, 552-554 (2011).

[13] Sahin, E., Ooi, K.J. A., Chen, G. F. R., Ng, D. K. T., Png, C. E., and Tan, D. T. H., "Enhanced optical nonlinearities in CMOS-compatible ultra-silicon-rich nitride photonic crystal waveguides," Appl. Phys. Lett. 110, 161113 (2017).
[14] Xing, P., Chen, G. F. R., Zhao, X., Tan, M. C. and Tan, D. T. H., "Silicon Rich Nitride Ring Resonators for rare-earth doped C-band amplifiers pumped at the O-band," Sci. Rep. 7, 9101 (2017).
[15] Sahin, E., Ooi, K. J. A., Png, C. E. and Tan, D. T. H., "Large, scalable dispersion engineering using cladding-modulated Bragg gratings on a silicon chip," Appl. Phys. Lett. 110, 161113 (2017).
[16] Chen, G. F. R., Wang, T., Donnelly, C., and Tan, D. T. H., "Second and third order dispersion generation using nonlinearly chirped silicon waveguide gratings," Opt. Express 21, 29223-29230 (2013).
[17] Li, J., White, T. P., O'Faolain, L., Gomez-Iglesias, A. and Krauss, T. F., "Systematic design of flat band slow light in photonic crystal waveguides," Opt. Express 16, 6227-6232 (2008).
[18] Debnath, A., Debnath, K. and O'Faolain, L., "Extraction of group index of lossy photonic crystal waveguides," Opt. Lett. 40, 193-196 (2015).